PAPER REF: 4626

# STATIC AND DYNAMIC SHAPE CONTROL OF LAMINATED BEAMS WITH RESISTEVELY INTERCONNECTED PIEZOELECTRIC PATCHES

**Juergen Schoeftner[1(*)], Gerda Buchberger[2]**
[1]Institute of Technical Mechanics, Johannes Kepler University, Linz, Austria
[2]Institute for Microelectronics and Microsensors, Johannes Kepler University, Linz, Austria
[(*)]*Email:* juergen.schoeftner@jku.at

## ABSTRACT

In this contribution an extended Bernoulli-Euler theory for a laminated beam hosting several resistively interconnected piezoelectric patches is presented. Based on this theory it is shown how to calculate the optimal reference voltage level and to design the attached resistive network, which connects the electrodes of the piezoelectric layers, if one intends to follow a certain trajectory of the lateral deformation (shape control) of a tip-loaded beam. If one tries to annihilate the harmonic vibrations along the beam axis, we show that the design criterion derived in the static case yields that vibrations are attenuated as long as an electrical time constant is small compared to the time constant of the harmonic excitation. This parameter involves the number of the piezoelectric patches, the piezoelectric capacitance and the resistances of the electric circuit. The proposed shape control method is also verified by a three-dimensional finite element calculation in ANSYS.

**Keywords:** beam modelling with piezoelectric patches, vibration control, electric circuit, shape control.

## INTRODUCTION

Piezoelectric transducers are widely used nowadays for active and passive vibration control, for structural health monitoring and for energy harvesting. One special topic of feedforward control is known under the term shape control. Shape control has been introduced by (Hafka, 1985), who calculated the optimal temperature distribution in order to minimize the distortions from its original shape. Such problems are so-called inverse mechanical problems where external forces and moments are computed to obtain a desired displacement field, see (Irschik, 2003). Solutions may not exist, but if they exist they might not be unique. One example is a clamped-clamped slender beam with a constant distribution of the piezoelectric layer. It can be shown that the beam will not vibrate, if an electric voltage is applied over the transducer electrodes, see (Hubbard, 1992), (Irschik, 2003) and (Irschik, 1998). This means that if a shaped layer is added to the constant layer, the response of the beam is only a consequence of the voltage-actuated shaped layer. Another example for shape control is given in (Agrawal, 1999), who minimized the integral of the quadratic difference between a desired and an achieved static deflection to obtain the optimized piezoceramics actuator locations and voltages. The concept of shape control can be also transmitted, of course with some limitations, to passive smart beams with attached electric circuits. In (Schoeftner, 2009 and 2011) two conditions for the piezoelectric transducers and for the electric network are given in order to compensate monofrequent harmonic vibrations caused by arbitrary external forces, force couples or distributed loads. This contribution deals with slender beams hosting spanwise constant piezoelectric transducers, which are also called piezoelectric patches. A further possibility to damp structural deformations is the use of one or several arrays of electrically interconnected piezoelectric transducers. These configurations when electrical impedances are in connection to adjacent transducers are treated in (Vidoli, 2000), (Porfiri, 2004) and (dell'Isola, 2011). Patch actuators can be easily glued onto an elastic system and the resistor network can be removed, easily changed or tuned in order to optimize the damping capabilities. Beam models with interconnected resistive electric circuits may be interpreted as the discretization of a piezoelastic beam with resistive electrodes, see (Schoeftner, 2013) and (Buchberger, 2013). The results of their extended beam theory are two coupled partial differential equations. The first one is an extension of the Bernoulli-Euler beam theory for a purely elastic beam by means of a voltage-depended term, and the second one is a diffusion equation for the voltage distribution, with the time-derivative of the lateral deflection as the source term. The theory is verified by three-dimensional finite element calculations for highly, moderately and hardly conductive electrodes.

This paper is structured as follows: first, an overview of the equations of motions of a smart slender beam with attached piezoelectric patches is given, where resistors are linked between their electrodes. Second, we present a general formulation how to design the electric circuit and the value for the reference voltage source, in order to achieve a certain displacement field for the bending vibrations of a beam in the static regime. In the end we demonstrate the correctness of our theory by several numerical examples: in the static limit, once the displacement is completely annihilated along the beam axis and then a certain displacement trajectory is prescribed. Finally it is shown that the design criterion for shape control with perfect displacement compensation, which has been derived for static external loads, may be also be approximately fulfilled for dynamically loaded beam, as long as a certain non-dimensional parameter, involving the number and the capacitances of the piezoelectric patches, the total resistance of the circuit and the excitation frequency, is small.

## MODELING OF PIEZOELECTRIC BEAMS WITH RESISTEVELY INTERCONNECTED PIEZOELECTRIC PATCHES

In this section we give in brief the basic differential equations of motion of a piezoelectric beam, when the electrodes of the piezoelectric transducers are connected to a resistive electric circuit. For a detailed derivation the reader is referred to (Schoeftner, 2011 and 2011b) and (Buchberger, 2013).

### Equations of motion (mechanical relations)

A cantilever beam equipped with eight piezoelectric patches at the upper and lower surfaces of the non-piezoelectric, elastic substrate is depicted in Fig.1. Only slender beams are considered, for which the Bernoulli-Euler assumption holds. The electrodes of the piezoelectric transducers are assumed to be ideal. The external ones, e.g. the electrodes of patch #1 and #2, are linked via the resistor $R_{12}$ (or i.e. via the impedance). It is assumed that the reference voltage source $V_0(t)$ is prescribed and that one end of the resistor (here $R_{89}$) is connected to ground $V_9 = 0\,\mathrm{V}$. Additionally, all inner electrodes are connected to ground. In the following the index $k$ stands for substrate (s), for piezo (p), or for lower and upper (l, u). If the location of the patches from the clamped boundary is the same for the upper and lower patches, if the material and geometrical properties (length $l_\mathrm{p}$ and height $h_k = z_{2k} - z_{1k}$) are equal, and if only loads $q_z(x)$ in the lateral direction act on the beam, but no compressive or tensile forces in the x-direction, the bending equation of motion for the deflection $w_0$ is decoupled from the axial equation of motion, and reads

$$M_w \ddot{w}_0 + K_\mathrm{M} w_{0,xxxx} = q_z(x). \tag{1}$$

The bending stiffness is $K_\mathrm{M} = K_\mathrm{M,elast} + K_\mathrm{M,piezo}$, where patch $n$ is located ($x_{an} < x < x_{an} + l_\mathrm{p}$), otherwise it only consists of the stiffness of the elastic substrate $K_\mathrm{M} = K_\mathrm{M,elast}$. In a similar manner this also holds for the mass per unit length $M_w = M_{w,\mathrm{elast}} + M_{w,\mathrm{piezo}}$. These quantities are calculated by

$$\begin{aligned} K_\mathrm{M}(x) &= K_\mathrm{M,elast}(x) + K_\mathrm{M,piezo}(x) = \sum_{k=\mathrm{s,u,l}} \tilde{C}_{11}^k \frac{z_{2k}^3 - z_{1k}^3}{3} b_k(x) + \sum_{k=\mathrm{u,l}} \frac{\left(\tilde{e}_{31}^k\right)^2 \left(z_{2k} - z_{1k}\right)^3}{12\tilde{\kappa}_{33}^k} b_k(x) \\ M_w(x) &= \sum_{k=\mathrm{s,u,l}} \int_{z_{1k}}^{z_{2k}} \rho_k b_k(x) \mathrm{d}z, \end{aligned} \tag{2}$$

with the density $\rho_k$, effective Young's modulus $\tilde{C}_{11}^k$, the transverse piezo-coefficient $\tilde{e}_{31}^k$ and the strain-free permittivity $\tilde{\kappa}_{33}^k$. The thickness coordinate and the width of the beam are denoted by $z_{2k}, z_{1k}$ and $b_k(x)$.

At $x_{an}$ and $\widehat{x}_{an} = x_{an} + l_\mathrm{p}$, which are the coordinates between a piezoelectric patch is located, the four continuity relations (deflection, rotation, bending moment and shear force) read[1]

$$\begin{aligned} & w_0(x_{an}^-) = w_0(x_{an}^+) \\ & w_{0,x}(x_{an}^-) = w_{0,x}(x_{an}^+) \\ & -K_\mathrm{M,elast} w_{0,xx}(x_{an}^-) = -\left(K_\mathrm{M,elast} + K_\mathrm{M,piezo}\right) w_{0,xx}(x_{an}^+) + 2\tilde{e}_{31} z_\mathrm{mp} b_\mathrm{p} V_n \\ & -K_\mathrm{M,elast} w_{0,xxx}(x_{an}^-) = -\left(K_\mathrm{M,elast} + K_\mathrm{M,piezo}\right) w_{0,xxx}(x_{an}^+) \end{aligned} \tag{3}$$

and

$$\begin{aligned} & w_0(\widehat{x}_{an}^-) = w_0(\widehat{x}_{an}^+) \\ & w_{0,x}(\widehat{x}_{an}^-) = w_{0,x}(\widehat{x}_{an}^+) \\ & -\left(K_\mathrm{M,elast} + K_\mathrm{M,piezo}\right) w_{0,xx}(\widehat{x}_{an}^-) + 2\tilde{e}_{31} z_\mathrm{mp} b_\mathrm{p} V_n = -K_\mathrm{M,elast} w_{0,xx}(\widehat{x}_{an}^+) \\ & -\left(K_\mathrm{M,elast} + K_\mathrm{M,piezo}\right) w_{0,xxx}(\widehat{x}_{an}^-) = -K_\mathrm{M,elast} w_{0,xxx}(\widehat{x}_{an}^+). \end{aligned} \tag{4}$$

[1] The limits from below (left) and from above (right) at $x_{an}$ are distinguished by $x_{an}^-$ and $x_{an}^+$, respectively.

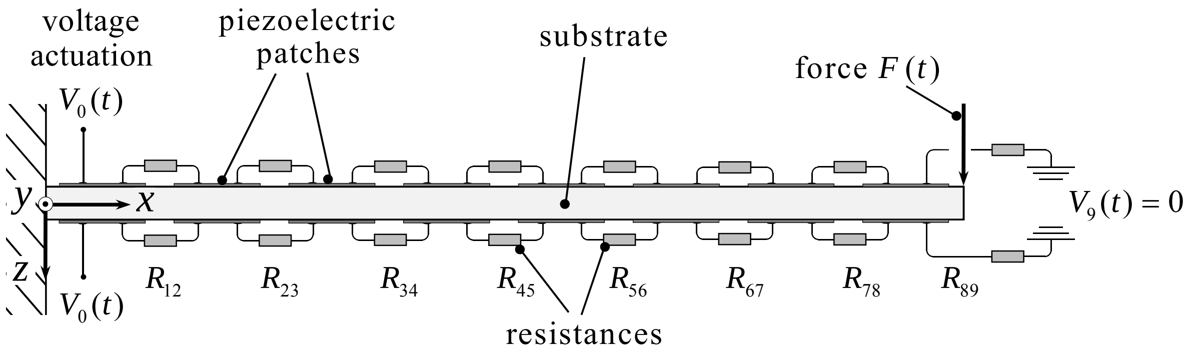


Fig.1 Sketch of a clamped-free beam with piezoelectric patches. The voltage $V_0(t)$ and the resistors $R_{ij}$ are the same for upper and lower side and cause a voltage distribution of the piezoelectric patches

**Electrical relations:**

Since the governing equation of motion (1) and its continuity relations (3) and (4) are coupled the electrical voltage of patch #*n*, also the influence of the mechanical deformation on the electrical relations has to be considered. It can be shown that the total charge over the external electrodes depends on the beam inclination at $x_{an}$ and $\hat{x}_{an} = x_{an} + l_{\mathrm{p}}$, and on the electrical voltage $V_n$ over the electrodes of each patch

$$\begin{aligned} Q_n &= Q_{n,\mathrm{elast}} - CV_n \qquad n = \{1,2,\ldots,N\} \\ Q_{n,\mathrm{elast}} &= -\tilde{e}_{31} z_{\mathrm{mp}} b_{\mathrm{p}} \left( w_{0,x}(\hat{x}_{an}) - w_{0,x}(x_{an}) \right), \quad C = \frac{\tilde{\kappa}_{33} b_{\mathrm{p}} l_{\mathrm{p}}}{h_{\mathrm{p}}}. \end{aligned} \tag{5}$$

Taking into advantage of Kirchhoff's current rule (KCR), which states that the sum of incoming and outcoming current is equal, one finds

$$i_{n\,n+1} - i_{n-1\,n} = \dot{Q}_n \qquad n = \{1,2,\ldots,N\} \tag{6}$$

In (6), $i_{mn}$ are the electric current from patch #*m* to patch #*n*, thus causing a voltage drop over the resistor $R_{mn}$. Applying Kirchhoff's voltage rule (KVR), one finds the connection between the electric current and the patch voltages

$$V_n - R_{n\,n+1}\, i_{n\,n+1} = V_{n+1} \qquad n = \{0,1,\ldots,N-1,N\} \tag{7}$$

For the numerical example, when a beam with eight piezoelectric patch actuators (*n*=8) is used, we find nine algebraic equations (KVR-(7)) and eight differential equations (KCR-(5) and (6)) in order to determine the eight unknown voltage drops $V_1, V_2, \ldots, V_8$ and nine unknowns for the current flow $i_{01}, i_{12}, \ldots, i_{78}, i_{89}$. This means, that from the electrical relation, the patch voltages are calculated, which also serves as an input source for the equation of motion and its continuity conditions (1), (3) and (4). The outcome of the mechanical part is the displacement field $w_0(x)$, which is needed in the charge equation for the electrical part, to ensure a fully-coupled electromechanical beam model within the framework of Bernoulli-Euler.

## DISPLACEMENT TRACKING OF A TIP-LOADED CANTILEVER

In this section we calculate the necessary voltage to be chosen for the reference signal $V_0$ and the proper values for the resistors $R_{ij}$, in order to achieve a certain lateral deflection in the static case, when the beam is subjected to an external load, force or force couple. One special goal of this displacement tracking problem is to completely annihilate the bending deformation at certain locations along the beam axis. We will show later on by the numerical example, that if one tries to eliminate the displacement, the design rules for the reference voltage and the resistor values might be also suitable values for a dynamically loaded beam.

In the static case, one can show that the deflection of a beam with arbitrary boundary conditions may be written as

$$w_0(x) = \sum_{m=1}^{M} G_{Fm}(x) F_m + \sum_{n=1}^{N} G_{Vn}(x) V_n \,. \tag{8}$$

The displacement $w_0(x)$ is a function of the external load vector $\underline{F} = \left[ F_1 \,, F_2 \,, \ldots , F_m \right]$ (this one may consist of either distributed loads, single force or force couples) and the voltage over the piezoelectric patches $\underline{V} = \left[ V_1 \,, V_2 \,, \ldots , V_n \right]$. The influence functions are denoted by $G_{Fm}$ and $G_{Vn}$, which might be found based on analytical considerations or might be the result of numerical approximation methods (e.g. for a beam with varying material properties, a stepped beam, etc… approximate solutions may be obtained by the Ritz or by a finite element method). If one uses *n* piezoelectric patches, it seems reasonable that the displacement at *n* different locations $x_{sj}$ might be arbitrarily chosen. Accounting for (8), one obtains in matrix notation

$$\underline{W}_0 = \underline{\underline{G}}_F \underline{F} + \underline{\underline{G}}_V \underline{V}, \tag{9}$$

where the matrices for the influence functions are written as

$$\begin{gathered}
\underline{\underline{G}}_F = \begin{pmatrix} G_{F1}(x_{s1}) & G_{F2}(x_{s1}) & G_{V3}(x_{s1}) & \cdots & G_{V8}(x_{s1}) \\ G_{F1}(x_{s2}) & G_{F2}(x_{s2}) & G_{V3}(x_{s2}) & \cdots & G_{V8}(x_{s2}) \\ \vdots & \vdots & \vdots & \ddots & \vdots \\ G_{F1}(x_{s8}) & G_{F2}(x_{s8}) & G_{V3}(x_{s8}) & \cdots & G_{V8}(x_{s8}) \end{pmatrix} \\
\underline{\underline{G}}_V = \begin{pmatrix} G_{V1}(x_{s1}) & G_{V2}(x_{s1}) & G_{V3}(x_{s1}) & \cdots & G_{V8}(x_{s1}) \\ G_{V1}(x_{s2}) & G_{V2}(x_{s2}) & G_{V3}(x_{s2}) & \cdots & G_{V8}(x_{s2}) \\ \vdots & \vdots & \vdots & \ddots & \vdots \\ G_{V1}(x_{s8}) & G_{V2}(x_{s8}) & G_{V3}(x_{s8}) & \cdots & G_{V8}(x_{s8}) \end{pmatrix}.
\end{gathered} \tag{10}$$

If the inverse matrix of $\underline{\underline{G}}_V$ exists[2], one solves (9) for the necessary patch voltage vector, which reads

$$\underline{V} = \underline{\underline{G}}_V^{-1} \left( \underline{W}_0 - \underline{\underline{G}}_F \underline{F} \right). \tag{11}$$

[2] This is a topic of ongoing research to find proper patch locations and sensor locations, such that the inverse matrix exist.

Due to practical reasons, it is advantageous to prescribe only one voltage signal, so we are not allowed to prescribe the voltage across all piezoelectric patches. From static considerations it is clear, that the piezoelectric patches, which behave like capacitances from an electrical point of view, totally block the direct-current, so the current passing the resistors is equal $i = i_{01} = i_{12} = \ldots = i_{89}$, and Kirchhoff's voltage rule (7) is simplified. The result is an equation for the parameters of the resistive network

$$\frac{V_{n-1} - V_n}{V_n - V_{n+1}} = \frac{R_{n-1\,n}}{R_{n\,n+1}} \qquad n = \{1, 2, \ldots, 7, 8\}. \tag{12}$$

## NUMERICAL RESULTS – STATIC DISPLACEMENT COMPENSATION

In this section, we show the correctness of our derived theory by a numerical experiment. Our aim is to annihilate the deflection of a tip-loaded cantilever beam equipped with eight equidistantly distributed piezoelectric patches (see Fig.1). The geometry and the material parameters of the configuration are given in Table 1. We compare the one-dimensional results obtained with the presented theory to three-dimensional finite elements results in ANSYS. For the one-dimensional model, the Bernoulli-Euler beam is discretized into 34 finite elements in the axial direction. As shape functions the well-known Hermite polynomials are used to discretize equation (1), which are then coupled to the charge equation of the electrodes, the Kirchhoff voltage and current rules (5), (6) and (7). For the 3D-ANSYS model, the beam is divided into 96 elements in the axial direction, 6 elements in the thickness direction and 8 elements in the thickness direction. The piezoelectric patches consist of 16, 4 and 8 elements in the axial, thickness and lateral direction. The electrodes are modelled by coupling the voltage degrees of freedom. The inner electrodes are kept at zero potential, whereas the electrical degrees of freedom of the external electrodes are coupled to CIRCU94 elements, which model the resistances $R_{ij}$. The coupled-field solid element SOLID5 is used for the substrate and also for the piezoelectric layers, since besides of three degrees of freedom for the displacement, it enables an additional degree of freedom for the electrical voltage.

Results for the static displacement, when the single load $F_0$=1N acts at the free end of the beam, for both the Bernoulli-Euler model (1d-BE) according to (1)-(7) and the ANSYS-model (3d-ANSYS), are given in Fig.2. The optimal reference voltage signal $V_0$=250.3V is calculated from (11) with $\underline{W}_0 = \underline{0}$

$$\underline{V}^T = [V_1, V_2, \ldots, V_8] = [250.3, 205.9, 184.9, 140.7, 120.0, 75.6, 54.8, 10.4]\,\mathrm{V}. \tag{13}$$

Substituting (13) into (12), one obtains the values for the resistive circuit, if one resistance or the sum of them is specified (Table 1).

Table 1 Values for the resistances of the circuit, when the deformation at the sensor locations $x_{si}$ should vanish. The sum of all resistors is $R_{tot}$=2000Ω

| resistance (unit) | value | resistance (unit) | value | resistance (unit) | value |
|---|---|---|---|---|---|
| $R_{01}(\Omega)$ | 0 | $R_{12}(\Omega)$ | 355.2 | $R_{23}(\Omega)$ | 167.4 |
| $R_{34}(\Omega)$ | 353.6 | $R_{45}(\Omega)$ | 165.6 | $R_{56}(\Omega)$ | 354.8 |
| $R_{67}(\Omega)$ | 166.0 | $R_{78}(\Omega)$ | 354.4 | $R_{89}(\Omega)$ | 83.0 |

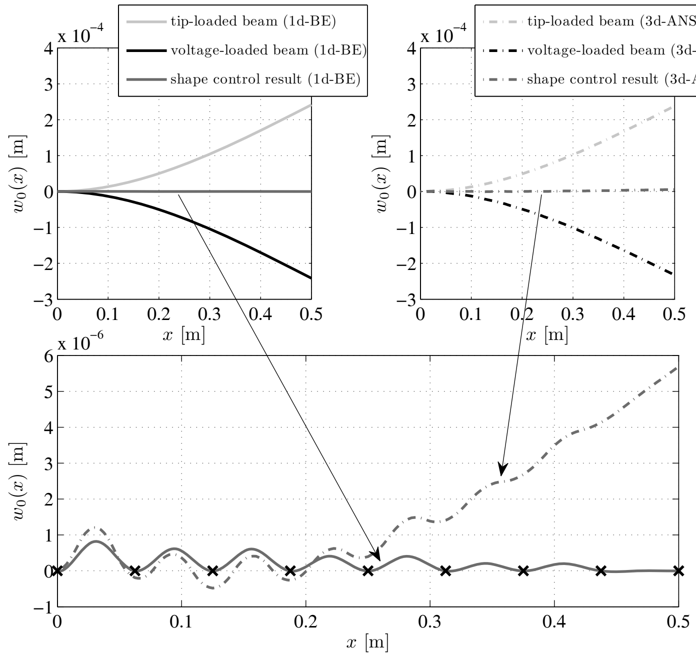


Fig.2 Static deflection of a tip-loaded beam with the Bernoulli-Euler and the 3d-ANSYS (light gray-only tip-force, black-only voltage load, dark gray-shape controlled beam) model

Fig.2 shows that the tip-deflections for the voltage-loaded and for the tip-loaded beam are the same, but opposite in sign $w_0(l) = \pm 0.24 \times 10^{-3}\,\mathrm{m}$ for the Bernoulli-Euler beam (top-left). Superposing both results yields that the displacement vanishes at the eight sensor locations

$$x_{si} = l \times i/8 \rightarrow \left[ x_{s1}, x_{s2}, x_{s3}, x_{s4}, x_{s5}, x_{s6}, x_{s7}, x_{s8} \right] = \left[1,2,3,4,5,6,7,8\right] \times \frac{0.5}{8}\,\mathrm{m}. \tag{14}$$

These locations are drawn by the black x-marks.

In ANSYS (top-right) a slight deviation occurs for the tip-loaded $w_0(l) = 0.238 \times 10^{-3}\,\mathrm{m}$ and the voltage-actuated beam $w_0(l) = -0.232 \times 10^{-3}\,\mathrm{m}$, therefore a residual deformation remains $w_0(l) = 5.7 \times 10^{-6}\,\mathrm{m}$, if both load possibilities are superposed.

## NUMERICAL RESULTS – STATIC DISPLACEMENT TRACKING

Now we generalize the above-derived results by demanding that the displacement vector should read

$$\underline{W}_0^T = \left[0,0,1,1,1,1,1,1\right] \times 10^{-6}\,\mathrm{m} \tag{15}$$

at the eight sensor locations $x_{si} = l \times i/8$, i.e. only the deformations at the first and the second sensor locations should vanish. For this, the necessary distribution of the actuation voltages is calculated from (11) and is no longer monotonically decreasing with respect to the x-coordinate

$$\underline{V}^T = \left[V_1, V_2, \ldots, V_8\right] = \left[250.5, 205.9, 138.9, 232.7, 27.9, 167.6, -37.3, 102.4\right]\mathrm{V} \tag{16}$$

As (16) shows the maximum voltage occurs at patch #1 with $V_1$=250.3V, followed by the patch #4 with $V_4$=232.7V , etc… This distribution is obtained by linking resistors between patch #1 and #4, denoted by $R_{14}$, then one resistance $R_{42}$ between patch #4 and #2, etc… The corresponding values for the resistances are given in Table 2. One sees that the first patch, which is actuated by the reference voltage $V_0$=250.3V, since $R_{01}$=0Ω holds and no voltage drop occurs, is also connected to the fourth patch due to $R_{14}$=122.4Ω. The forth patch is also linked to the second patch by $R_{42}$=186.7Ω and so on. The total sum of the resistances is the same as in the previous case $R_{tot}$=2000Ω, when no deformation should occur at the eight desired locations. The only difference to the previous configuration is that the terminal voltage is negative $V_7$=$V_9$=-37.3V. One sees from (16) that the voltage across the electrodes of the seventh patch are reversed in sign, i.e. that the electric potential of the external electrode is lower the one of the internal electrode.

Table 2 Values for the resistances of the circuit. The sum of all resistors is $R_{tot}$=2000Ω

| resistance (unit) | value | resistance (unit) | value | resistance (unit) | value |
|---|---|---|---|---|---|
| $R_{01}(\Omega)$ | 0.0 | $R_{14}(\Omega)$ | 122.4 | $R_{42}(\Omega)$ | 186.7 |
| $R_{26}(\Omega)$ | 266.1 | $R_{63}(\Omega)$ | 199.7 | $R_{38}(\Omega)$ | 253.5 |
| $R_{85}(\Omega)$ | 518.4 | $R_{57}(\Omega)$ | 453.2 | $R_{79}(\Omega)$ | 0.0 |

The result of this tracking problem is shown in Fig.3. The third to eight sensor locations are exactly $10^{-6}\,\mathrm{m}$ for the Bernoulli-Euler beam model.

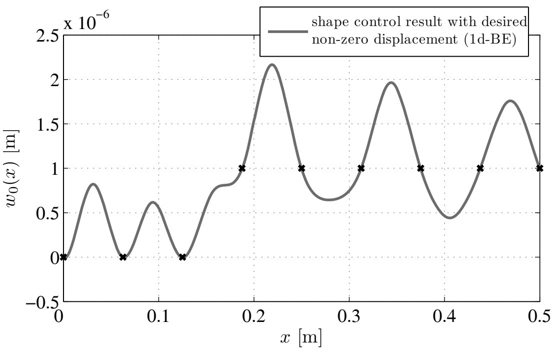


Fig.3 Static deflection of a tip-loaded beam with optimal reference voltage and the resistors from Table 2. The black marks indicate the target displacements to be tracked

## NUMERICAL RESULTS – DYNAMIC DISPLACEMENT COMPENSATION

In this section we ask if it is also possible annihilate or at least reduce the vibrations, when the cantilever beam is dynamically loaded $F(x,t) = F_0 \sin \omega t$. We will see that the values of the resistive circuit strongly affect the performance of our open-loop control technique. We use the same network configuration as in the static case, when the static deformations have been completely annihilated (Table 1). We compare these results with a system when the resistances are the tenfold of these values, so that the total resistance is increased from $R_{tot}$=2000Ω to $R_{tot}$=20kΩ.

First the results for $R_{tot}$=2000Ω are shown in Fig.4 (Bernoulli-Euler FE and ANSYS). If the shape control technique is applied (gray curve), the deflection at the free end approaches zero $\hat{w}_0(l,\omega \to 0) \to 0\,\mathrm{m}$ for low-frequency excitations, as it is expected from Fig.2. For higher frequencies the deflection is reduced by two orders of magnitude for frequencies below $f < 50\,\mathrm{Hz}$. The tip-deflections at the first natural frequency $f_1 = 26.5\,\mathrm{Hz}$ are $\hat{w}_0(l,\omega_1) = 9.0\times10^{-3}\,\mathrm{m}$ (tip-force) and only $\hat{w}_0(l,\omega_1) = 0.44\times10^{-3}\,\mathrm{m}$ with our proposed method (shape control), when the Bernoulli-Euler theory is used. Results from the three-dimensional ANSYS model are quite similar, the deformation at the resonance are reduced from $\hat{w}_0(l,\omega_1) = 9.3\times10^{-3}\,\mathrm{m}$ (tip-force) to $\hat{w}_0(l,\omega_1) = 0.43\times10^{-3}\,\mathrm{m}$ (shape control). The major differences to the one-dimensional Bernoulli-Euler results are that for low frequencies, the remaining tip-deflection does not vanish, when the shape control method is applied $\hat{w}_0(l,\omega_1) = 5.7\times10^{-6}\,\mathrm{m}$, (cf. static results from ANSYS results-Fig.2).

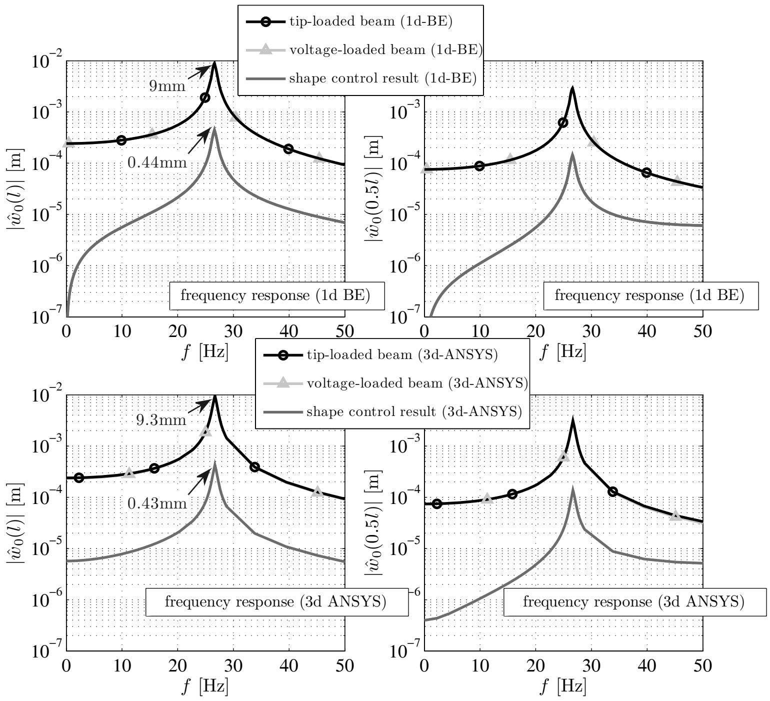


Fig.4 Frequency response $\hat{w}_0(l)$ (left) and $\hat{w}_0(0.5l)$ (right) with Bernoulli-Euler finite elements (top) and ANSYS (bottom) for the lower resistive circuit ($R_{tot}$=2000Ω) when the cantilever beam is excited by the tip-force excitation (black), by the voltage actuation (light gray) and by both the voltage and tip-force excitation (shape control-gray)

Results for the higher resistive circuit ($R_{tot}$=20kΩ) are shown in Fig.5 (Bernoulli-Euler FE). If the shape control technique is applied (gray curve), the deflection is also zero $\hat{w}_0(l,\omega\to0)\to0\,\mathrm{m}$ for excitations in the static limit. But for higher frequencies the deflection is not as strong attenuated as for the lower resistive circuit. The tip-deflections at the first natural frequency $f_1 = 26.5\,\mathrm{Hz}$ is $\hat{w}_0(l,\omega_1) = 8.2\times10^{-3}\,\mathrm{m}$ (tip-force) is lower, since the dissipated energy through the resistive shunt cannot be neglected (passive vibration control). With our proposed method, the remaining vibration at the free end is 34% of the uncontrolled motion and reads $\hat{w}_0(l,\omega_1) = 2.8\times10^{-3}\,\mathrm{m}$. Furthermore, it is obvious that the higher the frequency of the excitation signal, the less optimal is the higher-resistive circuit and the more inefficient is our shape control method. It can be derived from (5)-(7), see (Schoeftner, 2013), that a non-dimensional parameter $\pi_1$ exists, which determines if the shape control design will efficiently reduce structural vibrations or not

$$\pi_1 := O\left( CR_{\text{total}} \frac{\dot{V}_1 + \ldots + \dot{V}_8}{V_0} \right) = 8CR_{\text{total}}\omega = \tau\omega. \tag{17}$$

In (17) the electrical time constant is denoted by $\tau = 8CR_{\text{total}}$, and depends on the number of piezoelectric patches, the total resistance of the circuit and the mean capacitance of the piezoelectric patch. In case of a low excitation frequency $\omega \to 0$ or of a low resistive electrical circuit $R_{\text{total}} \to 0$, the proposed control method strongly reduces vibrations. If $\pi_1 \gg 1$ holds, vibrations will only be slightly reduced (see Fig.5) or, in the worst case, even amplified.

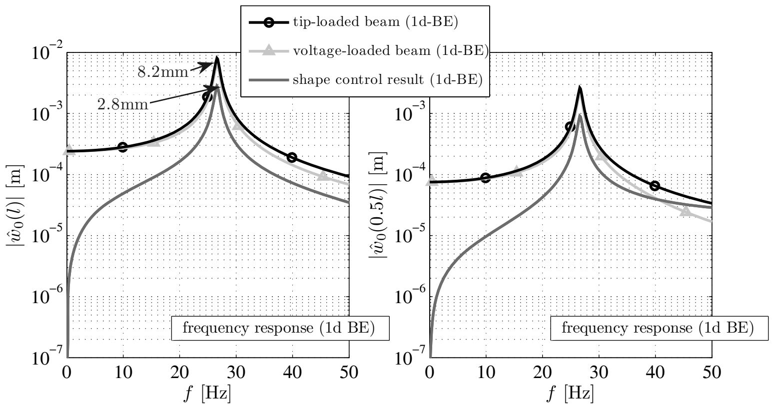


Fig.5 Frequency response $\hat{w}_0(l)$ (left) and $\hat{w}_0(0.5l)$ (right) with Bernoulli-Euler finite elements for the higher resistive circuit ($R_{tot}$=20kΩ) when the cantilever beam is excited by the tip-force excitation (black), by the voltage actuation (light gray) and by both the voltage and tip-force excitation (shape control-gray)

## CONCLUSION

In this contribution we presented a new method how to control vibrations of elastic slender beam-type structures. This is known under shape control in the literature. First the basic mechanical and electrical relations for a slender beam within the framework of Bernoulli-Euler, which is equipped with piezoelectric patches, whose electrodes are connected to a resistive circuit, are presented. Then an analytical expression for the lateral deflection of a beam is given, which uses so-called influence functions of the force-loaded beam and the voltage-loaded piezoelectric patches. If the displacements of *n* arbitrary locations along the beam length are to be controlled, one can achieve this by a proper actuation of *n* piezoelectric control agencies, by inverting the set of linear equations relating the displacement, the force load and the voltage actuation. The correctness of our theory, when a certain trajectory is prescribed in the static regime and the vibrations are to be attenuated in the dynamic regime, is shown by one-dimensional results using Bernoulli-Euler elements and also by a three-dimensional electromechanically-coupled finite element calculation performed in ANSYS.

## ACKNOWLEDGMENTS

The research was funded by the COMET K2-Center ACCM and the Austrian Research Promotion Agency (FFG) under the contract number 825348/K-Licht.

## Appendix A

For the numerical case study the material parameters and the geometrical dimensions (Aluminum for the substrate with index s, PZT-5A for the piezoelectric patch with index p) are listed in Table 3. The effective piezomodulus, the modulus of elasticity and the strain-free permittivity are obtained from the values (listed in the following) by taking advantage of the transformation rules, see (Schoeftner, 2011b).

Material properties of PZT-5A:

- Density: $\rho_\mathrm{p} = 7750\,\mathrm{kgm^{-3}}$
- Elasticity components in Voigt notation: $C_{11} = C_{22} = 123\times10^9\,\mathrm{Nm^{-2}}$, $C_{12} = 76.7\times10^9\,\mathrm{Nm^{-2}}$, $C_{13} = C_{23} = 70.3\times10^9\,\mathrm{Nm^{-2}}$, $C_{33} = 97.1\times10^9\,\mathrm{Nm^{-2}}$, $C_{44} = C_{55} = 22.3\times10^9\,\mathrm{Nm^{-2}}$, $C_{66} = 0.5\left(C_{11} - C_{12}\right) = 23.15\times10^9\,\mathrm{Nm^{-2}}$, else $C_{ij} = 0\,\mathrm{Nm^{-2}}$
- Components of piezoelectric modulus in Voigt notation: $e_{31} = e_{32} = -7.15\,\mathrm{Asm^{-2}}$, $e_{33} = 13.7\,\mathrm{Asm^{-2}}$, $e_{24} = e_{15} = 11.9\,\mathrm{Asm^{-2}}$, else $e_{ij} = 0\,\mathrm{Asm^{-2}}$
- Components of permittivity in Voigt notation: $\kappa_{11} = \kappa_{22} = 1649\times\varepsilon_0$, $\kappa_{33} = 1750\times\varepsilon_0$ with $\varepsilon_0 = 8.854\times10^{-12}\,\mathrm{AsV^{-1}m^{-1}}$, else $\kappa_{ij} = 0\,\mathrm{AsV^{-1}m^{-1}}$

Table 3 Parameters used in the numerical example

| variable (unit) | value | variable (unit) | value |
|---|---|---|---|
| $\rho_\mathrm{p}\left(\mathrm{kgm^{-3}}\right)$ | 7750 | $\rho_\mathrm{s}\left(\mathrm{kgm^{-3}}\right)$ | 2700 |
| $z_{1\mathrm{p}}\left(\mathrm{m}\right)$ | $4.00\times10^{-3}$ | $z_{2\mathrm{p}}\left(\mathrm{m}\right)$ | $4.40\times10^{-3}$ |
| $z_{1\mathrm{s}}\left(\mathrm{m}\right)$ | $-4.00\times10^{-3}$ | $z_{2\mathrm{s}}\left(\mathrm{m}\right)$ | $4.00\times10^{-3}$ |
| $l\left(\mathrm{m}\right)$ | 0.5 | $l_\mathrm{p}\left(\mathrm{m}\right)$ | 0.03 |
| $\tilde{\kappa}_{33}^{\mathrm{p}}\left(\mathrm{AsV^{-1}m^{-1}}\right)$ | $2.15\times10^{-8}$ | $\tilde{e}_{31}^{\mathrm{p}}\left(\mathrm{Asm^{-2}}\right)$ | $-10.94$ |
| $\tilde{C}_{11}^{\mathrm{p}}\left(\mathrm{Nm^{-2}}\right)$ | $6.29\times10^{10}$ | $\tilde{C}_{11}^{\mathrm{s}}\left(\mathrm{Nm^{-2}}\right)$ | $7.22\times10^{10}$ |
| $x_{\mathrm{a}i}\left(\mathrm{m}\right)$ | $0.01625 + l\times\left(i-1\right)/8$ | $x_{\mathrm{s}i}\left(\mathrm{m}\right)$ | $l\times i/8$ |
| $b_\mathrm{s}\left(\mathrm{m}\right)$ | 0.05 | $b_\mathrm{p}\left(\mathrm{m}\right)$ | 0.05 |
| $C\left(\mathrm{AsV^{-1}}\right)$ | $8.05\times10^{-8}$ | $F_0\left(\mathrm{N}\right)$ | 1 |

## REFERENCES

Agrawal B N, and Treanor K E. Shape control of a beam using piezoelectric actuators. Smart Mater. Struct., 1999, 8, p. 729-40.

Buchberger G, Schoeftner, J. Modeling of slender laminated piezoelastic beams with resistive electrodes - comparison of analytical results with three-dimensional finite element calculations. Smart Mater. Struct., 2013, 22, 032001 (13pp).

dell'Isola F, Maurini C, Porfiri M. Passive damping of beam vibrations through distributed electric networks and piezoelectric transducers: prototype design and experimental validation. Smart Mater. Struct., 13, 2011, p. 299-308.

Hafka R T, Adelman H M. An analytical investigation of shape control of large space structures by applied temperatures. AIAA Journal, 1985, 23, p. 450-57.

Hubbard J E, Burke S E. Distributed transducer design for intelligent structural components. in: Intelligent Structural System, H. S. Tzou and G. L. Anderson (eds.), Kluwer Academic Publishers, Norwell, 1992.

Irschik H, Krommer M, Belyaev A K, Schlacher K. Shaping of piezoelectric sensors/actuators for vibrations of slender beams: coupled theory and inappropriate shape functions. J. Intell. Mater. Syst. Struct, 1998, 9, p. 546-54.

Irschik H, Krommer M, Pichler U. Dynamic shape control of beam-type structures by piezoelectric actuation and sensing. Int. J. Appl. Electrom. Mechanics, 2003, 17, p. 251-58.

Porfiri M, dell'Isola F. Multimodal beam vibration damping exploiting PZT transducers and passive distributed circuits. J. Phys. IV, 2004, 115, p. 323-30.

Schoeftner J, Irschik H. Passive damping and exact annihilation of vibrations of beams using shaped piezoelectric layers and tuned inductive networks. Smart Mater. Struct., 2009, 18, 125008 (9pp).

Schoeftner J, Irschik H. Passive shape control of force-induced harmonic lateral vibrations for laminated piezoelastic Bernoulli-Euler beams-theory and practical relevance. Smart Structures and Systems, 2011, 7, p. 417-32.

Schoeftner J, Irschik H. A comparative study of smart passive piezoelectric structures interacting with electric networks: Timoshenko beam theory versus finite element plane stress calculations. Smart Mater. Struct., 2011b, 20, 025007 (13pp).

Schoeftner J, Buchberger G. Active shape control of a cantilever by resistively interconnected piezoelectric patches. Smart Structures and System, 2013 (submitted for publication)

Vidoli S, dell'Isola F. Modal coupling in one-dimensional electro-mechanical structured continua. Acta Mech., 2000, 141, p. 37-50.